Comparative Analysis of Backstepping and Active Disturbance Rejection Control Approach used in Photovoltaic System Connected to the Grid

Youssef Barradi[**‡], Naoufel Khaldi[*], Khalida Zazi[**], Malika Zazi[**]

[*]Department of Electrical Engineering, Mohammadia School of Engineer, Mohamed V University, Rabat, Morocco

[**]Department of Electrical Engineering, Higher School of Technical Education, Mohammed V University, Rabat, Morocco

youssef.barradi@um5s.net.ma, naoufelkhaldi@gmail.com, zazikhalida@gmail.com, m.zazi@um5s.net.ma

[‡]Corresponding Author, Youssef Barradi, Department of Electrical Engineering, Higher School of Technical Education, Mohammed V University, Rabat, Morocco, Tel: +212642131667, youssef.barradi@um5s.net.ma

Received: xx.xx.xxxx Accepted: xx.xx.xxxx

Abstract- The aim of this paper is to ensure high performances of grid connected photovoltaic power system using DC-AC power inverters. It is susceptible to power grid disturbance, sudden environment changes and parameters uncertainties. Based in this characteristic, comparison between robust Backstepping controller and active disturbance rejection control (ADRC) strategy are developed. The two control algorithms are required to extract the maximum power of the solar energy, to maintain constant the DC-bus voltage, and to inject a suitable current into the grid with power factor near unity. Therefore, the Analysis and simulation of the ADRC and Backstepping controllers are validated with MATLAB/ Simulink software. It is showed the superiority of the backstepping technique through simulation results. Otherwise, The ADRC has only two parameters design, which make it easy to implement.

Keywords ADRC controller, Backstepping controller, MPPT, Photovoltaic system, Power grid.

Nomenclature and Acronyms :

i_{pv}	PV current module
E_g	band-gap energy of the semiconductor
I_{ph}	photocurrent PV module
T_{ref}	cell reference temperature (°K)
I_{rs}	reverse saturation current
MPPT	maximum power point tracking
I_{sc}	short circuit current per cell
PV	photovoltaic panel
n_p	number of solar cells connected in parallel
DT	differentiator trackers
n_s	number of solar cells connected in series
ESO	extended state observer
p	p–n junction ideality factor
FC	feedback controller
k	Boltzmann's constant (1.3806503 10-23 J/K)
DC	direct current
E	solar irradiance
ADRC	active disturbance rejection control
q	charge of an electron (q= 1.610-19 C)
AC	alternative current
T	cell temperature (°K)
PID	proportional integral derivative controller
V_{pv}	PV voltage module
UPFC	unity power factor controller
K	the temperature coefficient for short-circuit current
PWM	pulse with modulation

1. Introduction

In the recent years, solar energy became a famous clean energy source. The solar energy source systems are quickly growing thanks to the innovations and the researches in solar energy technology for electrical power production [1,2]. Since long time ago, fossil fuels have served as the major source of generating electrical energy. However, the transfer of energy from photovoltaic conversion system is adopted. Silent, clean and locally available, for these reasons solar plant can take advantage over conventional sources of energy.

To obtain an efficient electrical energy from the PV panels, the power electronic system which contain converters must be designed and controlled effectively to assure a high accuracy of the PV system. Therefore, many tracking control strategies have been proposed in existing literatures, such as perturb and observe, incremental conductance, neural network, and fuzzy logic methods, etc [2,3,17].

Referring to [4,5], PV energy application can be divided into two modes, that is the stand-alone PV system and the PV grid-connected system. This paper focuses in how to control the PV grid-connected system to deliver a high-quality power to the utility grid. According to [5,6], a lot of research are made to ensure a good transfer of energy and eliminate the harmonics distortion of current and voltage. However, the schemes proposed in these studies present some shortcomings and requires complex computations in the mathematical system model which influence implementation in reality.

This work presents a comparison between a backstepping method and new ADRC control technique which are two key methods used to design a suitable control for two stages of the PV grid connected system. This stage is composed with DC-AC inverters [16,18]. Backstepping method provides a recursive approach in the sense that it has a systematic way of constructing the Lyapunov function along with the control input design [7]. The design tool achieves the control objectives i.e. power tracking and robustness due to external climatic variation. In other way, the technique offers a choice of design for dwelling of some uncertain nonlinearity and can avoid undesired cancellations comparing to feedback linearization which cancels some useful nonlinearity.

In the other hand, ADRC method is a new technology for estimating and compensating uncertainties and disturbances, which have been explored and used recently as an alternative over classical techniques and especially PID controller [8,9]. Unlike many existing control methods, the ADRC does not require the accurate mathematical model of the plant [10]. Moreover, selecting the plant order n of the ADRC is quite flexible which make this control more convenient to apply in many control systems [12]. The method involves three blocks: differentiator Trackers (DT), Feedback controller (FC), and Extended state Observer (ESO) which is the main part of the command.

In detail, the suggested design techniques propose an evaluation to achieve three objectives. First one, is to control the converter in order to achieve maximum power point (MPP) even with variation of atmospheric conditions. Second, is to ensure the regulation of the DC link voltage. The Third is to deliver a sinusoidal current via DC-AC power system to the grid with a unity power factor. The control inputs are the duty cycles of the inverters. Simulation is made in different temperature and irradiation. Results provided show clearly the feasibility and the robustness of the proposed two techniques. They present also a good characteristic, excellent output from the nonlinear backstepping control comparing with ADRC command. The sequential work flow of this paper is as follows: In section II, complete system overview has been described. Section III covers both ADRC and Backstepping control design, followed by discussion on simulation results in section IV. Lastly, in section V, a conclusion has been added to finalize the work.

2. Complete System Overview

The complete two stages power system block is shown in Fig. 1. The energy captured by the PV will be supplied through the boost converter which will be controlled by a maximum power point tracking (MPPT) controller. After that, throughout DC link voltage and by changing the duty cycle of switching inverter, a power is delivered to the grid via single phase DC-AC inverter which contribute to reduce the harmonic content of the network current and assure unity power factor.

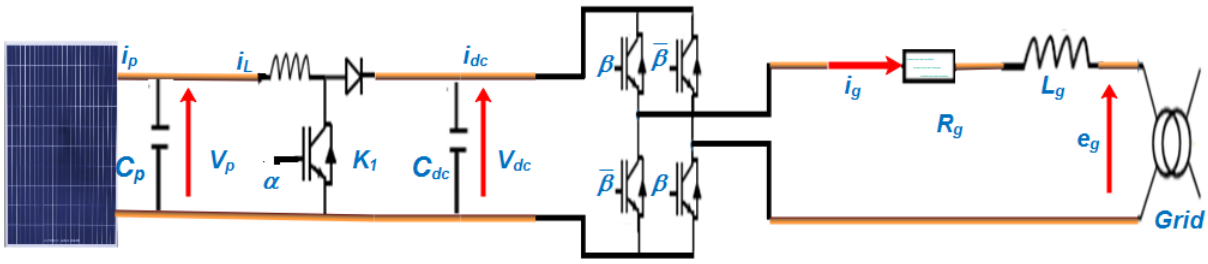

Fig.1. PV single-phase grid-connected system

2.1 Solar panels characteristics

Parameters of solar panel are shown in table I. PV module is made by solar company and product name is MLP-070P.

Table 1. Parameters of MLP-070P

Parameters	Values
Open Circuit Voltage(Voc)	23.5Volt
Short Circuit Current(Isc)	4.25Amp
Voltage at Pmax(Vmpp)	17.9Volt
Current at Pmax(Impp)	3.9Amp
Maximum Power (Pmpp)	70Watt

There are various methods to perform modeling work on the PV module, the most of them is described by using mathematical modeling [8,9]. To resolve the nonlinearity of current/voltage (*I-V*) characteristics of PV module, numerical method called Newton-Raphson is used to determine the operational point [3].

According to [3,4]. The one diode model of the PV panel is:

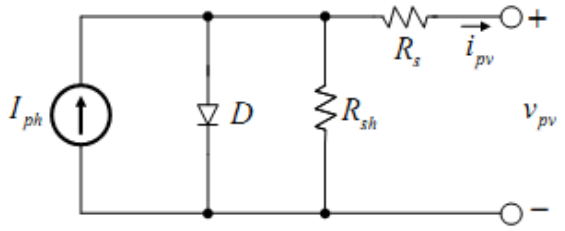

Fig. 2. The equivalent circuit of a photovoltaic array

The system is described by several equations below, meaning of the parameters expressed can be consulted in [4].

$$i_{pv} = n_p I_{ph} - n_p I_{rs}\left[\exp\left(\frac{q}{pkn_s}\times\frac{vpv}{T}\right) - 1\right] \quad (1)$$

$$I_{rs} = I_r(T/T_{ref})^3 \exp\left\{\left(\frac{qE_g}{pk}\right)\left(\frac{1}{T} - \frac{1}{T_{ref}}\right)\right\} \quad (2)$$

$$I_{ph} = [(I_{sc} + K(T - T_{ref})] \times \left(\frac{E}{E_r}\right) \quad (3)$$

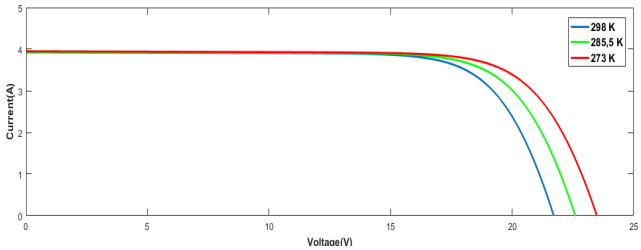

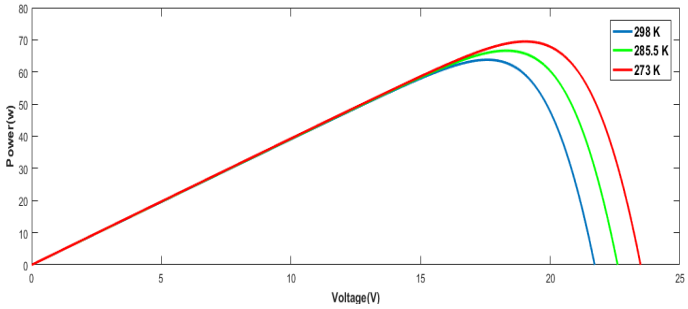

Fig. 3. Effect of temperature change in PV

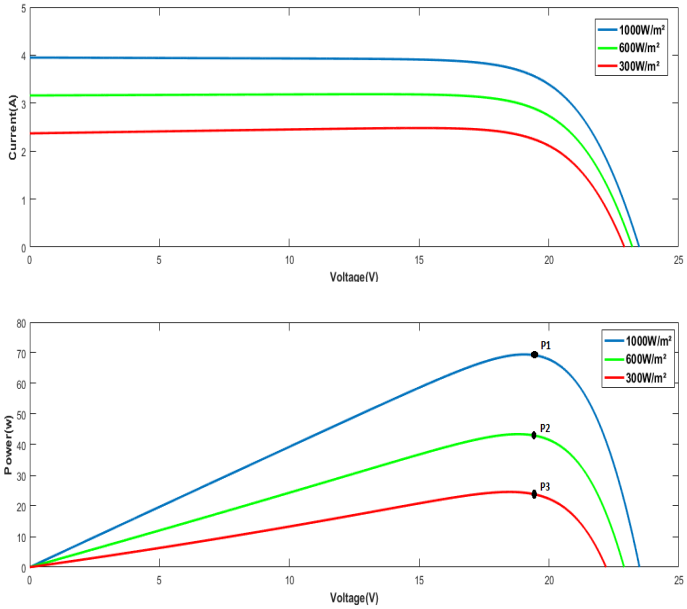

Fig. 4. Effect of irradiation change in PV

2.2 Power electronics inverters modeling

As can be seen in figure 1, the DC-DC boost converter contain a transistor controlled by a pulse with modulation (PWM) signal α, and the full bridge inverter where the four switches {K21; K22 ;K23 ;K24} can be IGBT or MOSFET is controlled by an input signal β:

$$\alpha = \begin{cases} 0\,; K1\ is\ ON \\ 1; K2\ is\ OFF \end{cases}$$

$$\beta = \begin{cases} 0; K21\ and\ K24\ are\ ON, K22\ and\ K23\ are\ OFF \\ 1; K22\ and\ K23\ are\ ON, K21\ and\ K24\ are\ OFF \end{cases}$$

Kirchhoff law's is applied to the power electronics circuit. If the switching frequency is high, an average mathematical model using grid connected PV is obtained to describe the dynamical behavior [11,15].

$$\begin{cases} \frac{dv_{pv}}{dt} = \frac{1}{C_{in}}(i_{pv} - i_L) \\ \frac{di_L}{dt} = \frac{v_{pv}}{L} - \frac{R}{L}i_L - \frac{V_{bat}}{L}(1 - \boldsymbol{\alpha 1}) \\ \frac{dv_{dc}}{dt} = \frac{i_L}{C_{dc}}(1 - \boldsymbol{\alpha 1}) - \frac{i_L}{C_{dc}}(2\boldsymbol{\beta 1} - 1) \\ \frac{di_g}{dt} = \frac{v_{dc}}{L_g}(2\boldsymbol{\beta 1} - 1) - \frac{R_g}{L_g}i_g - \frac{e_g}{L_g} \end{cases} \quad (4)$$

Table 2. Averaged Variables.

Variable	Averaged variable in (4)
PV voltage	v_{pv}
PV current	i_{pv}
Inductor current	i_L
DC bus voltage	v_{dc}
grid voltage	e_g
grid current	i_g
DC link capacitor	C_{dc}
input capacitor	C_{in}
filter inductor	L_g
resistance of the filter inductor	R_g

α1 and *β1* are the switching signals of the duty cycles input control *α* and *β*.

3. Proposed Controller Design

As shown in figure 5, the structure of the proposed single-phase grid connected system is presented. A comparison between ADRC technique and Backstepping method is developed to ensure the three aims enumerated in section I. In detail, there is functional MPPT controller even with climatic changes, the PI controller to regulate DC link voltage, and unity power factor controller (UPFC) to transfer high quality power.

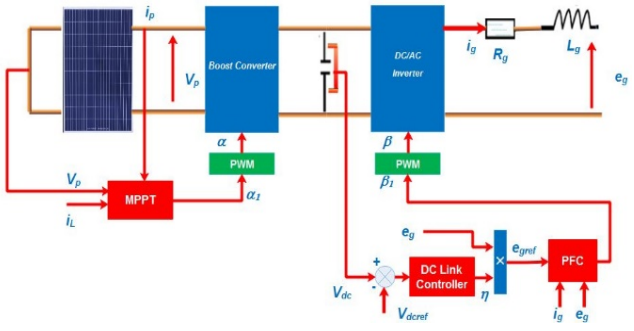

Fig. 5. Single grid power system

3.1 MPPT Backstepping Controller

Backstepping proposes a systematic synthesis method for the class of nonlinear systems having a triangular shape. It is based on the decomposition of the entire control system, which is generally multi-variable and high-order into a cascade of first-order control subsystems [7].

For each subsystem, a so-called virtual control law is calculated. The latter will serve as a reference for the next subsystem until obtaining the control law for the complete system.

The determination of the control laws that follows from this approach is based on the use of Lyapunov functions.

The main object is to extract the maximum power even with climatic changes. For that, a duty cycle α is obtained using the backstepping method. For controller design, the appropriate signal is used to regulate an output $z_1 = \frac{\partial P}{\partial v_{pv}}$ to its reference $z_{1ref} = \frac{\partial P}{\partial v_{pv}}\Big|_{MPP} = 0$ which guarantee that the PV system works at MPP.

Two design steps using the nonlinear backstepping controller were adopted.

Step 1

Let us show you the following tracking error:

$$e_1 = z_1 - z_{1ref}$$

Where

$$z_{1ref} = \frac{\partial P}{\partial v_{pv}}\Big|_{MPP} = \frac{\partial(v_{pv}i_{pv})}{\partial v_{pv}} = I_{pv} + v_{pv}\frac{\partial i_{pv}}{\partial v_{pv}} = 0 \quad (5)$$

Using 4 and 5, its dynamic is given by :

$$\dot{e}_1 = \left[i_{pv} + \frac{\delta i_{pv}}{\delta v_{pv}}v_{pv}\right]\ddot{v}_{pv}\frac{\delta t}{\delta v_{pv}} + \left[\frac{\delta i_{pv}}{\delta v_{pv}} + \frac{\partial^2 i_{pv}}{\partial^2 v_{pv}}v_{pv} + \frac{\delta i_{pv}}{\delta v_{pv}}\right]\left[\frac{1}{C_{in}}(i_{pv} - i_L)\right] \quad (6)$$

Consider the candidate Lyapunov function:

$$V_1 = \frac{1}{2}e^2{}_1$$

As its derivative with respect to time is:

$$\dot{V}_1 = e_1\left[i_{pv} + \frac{\delta i_{pv}}{\delta v_{pv}}v_{pv}\right]\ddot{v}_{pv}\frac{\delta t}{\delta v_{pv}} + \left[\frac{\delta i_{pv}}{\delta v_{pv}} + \frac{\partial^2 i_{pv}}{\partial^2 v_{pv}}v_{pv} + \frac{\delta i_{pv}}{\delta v_{pv}}\right]\left[\frac{1}{C_{in}}(i_{pv} - i_L)\right] \quad (7)$$

The choice $-C_1 e_1 = \dot{e}_1$ with $C_1 > 0$ is a design parameter whose dynamics is negative definite.

$$-C_1 e_1 = \left[i_{pv} + \frac{\delta i_{pv}}{\delta v_{pv}}v_{pv}\right]\ddot{v}_{pv}\frac{\delta t}{\delta v_{pv}} + \left[\frac{\delta i_{pv}}{\delta v_{pv}} + \frac{\partial^2 i_{pv}}{\partial^2 v_{pv}}v_{pv} + \frac{\delta i_{pv}}{\delta v_{pv}}\right]\left[\frac{1}{C_{in}}(i_{pv} - \mathbf{X_1})\right] \quad (8)$$

Where $\boldsymbol{X_1} = (i_L)_d$ is chosen as a virtual control, we can find the following stabilizing function:

$$\mathbf{X_1} = i_{pv} + \left(C_{in} \frac{1}{\left[\frac{\delta i_{pv}}{\delta v_{pv}} + \frac{\partial^2 i_{pv}}{\partial^2 v_{pv}} v_{pv} + \frac{\delta i_{pv}}{\delta v_{pv}}\right]} \right) \left(C_1 e_1 + \left(\left[i_{pv} + \frac{\delta i_{pv}}{\delta v_{pv}} v_{pv} \right] \ddot{v}_{pv} \frac{\delta t}{\delta v_{pv}} \right) \right) \quad (9)$$

Step 2

To achieve the control aim, new error variable of the boost inductor current is defined $e_2 = i_L - X_1$ which must be vanish. Combining (4) and (6), a control signal $\boldsymbol{\alpha 1}$ appeared.

$$\dot{e}_2 = \frac{v_{pv}}{L} - \frac{R}{L} i_L - \frac{V_s}{L}(1 - \boldsymbol{\alpha 1}) - \dot{X}_1 \quad (10)$$

$$\dot{e}_1 = \left[i_{pv} + \frac{\delta i_{pv}}{\delta v_{pv}} v_{pv} \right] \ddot{v}_{pv} \frac{\delta t}{\delta v_{pv}} + \left[\frac{\delta i_{pv}}{\delta v_{pv}} + \frac{\partial^2 i_{pv}}{\partial^2 v_{pv}} v_{pv} + \frac{\delta i_{pv}}{\delta v_{pv}} \right] \left[\frac{1}{C_{in}} (i_{pv} - (e_2 + X_1)) \right] \quad (11)$$

Adding (9), we define $\dot{e}_1$ and $\dot{V}_1$:

$$\dot{e}_1 = -\frac{1}{C_{in}} \left[\frac{\delta i_{pv}}{\delta v_{pv}} + \frac{\partial^2 i_{pv}}{\partial^2 v_{pv}} v_{pv} + \frac{\delta i_{pv}}{\delta v_{pv}} \right] e_2 - C_1 e_1 \quad (12)$$

$$\dot{V}_1 = -\frac{1}{C_{in}} \left[\frac{\delta i_{pv}}{\delta v_{pv}} + \frac{\partial^2 i_{pv}}{\partial^2 v_{pv}} v_{pv} + \frac{\delta i_{pv}}{\delta v_{pv}} \right] e_2 e_1 - C_1 e^2{}_1 \quad (13)$$

The derivative time of stabilizing function $\dot{X}_1$ is:

$$\dot{X}_1 = \left[\frac{\partial i_{pv}}{\partial t} \left(\frac{(C_1 \dot{e}_1 + e_1)}{\left(\frac{\delta i_{pv}}{\delta v_{pv}} + \frac{\partial^2 i_{pv}}{\partial^2 v_{pv}} v_{pv} + \frac{\delta i_{pv}}{\delta v_{pv}} \right)} - \frac{(C_1 e_1)}{\left(\frac{\delta i_{pv}}{\delta v_{pv}} + \frac{\partial^2 i_{pv}}{\partial^2 v_{pv}} v_{pv} + \frac{\delta i_{pv}}{\delta v_{pv}} \right)^2} \left(2 \frac{\delta^2 i_{pv}}{\delta v^2{}_{pv}} + \frac{\partial^3 i_{pv}}{\partial v^3{}_{pv}} v_{pv} + \frac{\delta^2 i_{pv}}{\delta v^2{}_{pv}} \right) \frac{\partial v_{pv}}{\partial t} \right) \right] \quad (14)$$

Consider the augmented candidate Lyapunov function:

$$V_2 = V_1 + \frac{1}{2} e^2{}_2$$

Time derivative of V_2 is given by:

$$\dot{V}_2 = e_2 \left[-\frac{1}{C_{in}} \left(\frac{\delta i_{pv}}{\delta v_{pv}} + \frac{\partial^2 i_{pv}}{\partial^2 v_{pv}} v_{pv} + \frac{\delta i_{pv}}{\delta v_{pv}} \right) e_1 + \frac{1}{L} (R - v_{pv} - v_{bat}) + \frac{v_{bat}}{L} \boldsymbol{\alpha 1} - \dot{X}_1 \right] - C_1 e^2{}_1 \quad (15)$$

We deduce the backstepping control law $\boldsymbol{\alpha 1}$ which guarantees the global stability:

$$\boldsymbol{\alpha 1} = \frac{L}{v_{bat}} \left[-\frac{1}{C_{in}} \left(\frac{\delta i_{pv}}{\delta v_{pv}} + \frac{\partial^2 i_{pv}}{\partial^2 v_{pv}} v_{pv} + \frac{\delta i_{pv}}{\delta v_{pv}} \right) e_1 - \frac{1}{L} (R - v_{pv} - v_{bat}) + \dot{X}_1 - C_2 e_2 \right] \quad (16)$$

Where $C_2 > 0$ is a design parameter, whose dynamics Lyapunov function is negative definite because:

$$\dot{V}_2 = -C_1 e^2{}_1 - C_2 e^2{}_2 < 0 \quad (17)$$

Then, the error is forced to converge asymptotically to the origin based in Lyapunov theory, which means $z_1 = \frac{\partial P}{\partial v_{pv}}$ converges to its reference $z_{1ref} = \frac{\partial P}{\partial v_{pv}} \Big|_{MPP} = 0$. Therefore, the MPP has been reached.

3.2 UPFC Controller

To attain the unity power factor, two cascaded control loops are designed. The output current inner loop which in charge to generate a sinusoidal converter output current in phase with the grid supply voltage, ensuring also current harmonics rejection. In other way, the control loop of the input voltage that regulate DC bus voltage at its reference value and deliver also the amplitude reference of the current PV Panel to the output inner loop. This inner loop guarantees that the grid reference signal i_{gref} will be reached by the grid current i_g.

$$i_{gref} = \eta e_g = \eta A \sin(\omega t) \quad (18)$$

η is a positive parameter adjusted by the following PI control law:

$$\eta(t) = C_3 \left(V_{dc}(t) - V_{dcref}(t) \right) + C_4 \int_0^t \left(V_{dc}(\tau) - V_{dcref}(\tau) \right) d\tau \quad (19)$$

Where C_3: the proportional gain
C_4: the integral gain

Let us introduce you the following current error:

$$e_3 = z_2 - z_{2ref} \quad (20)$$

Using (4) and (20), its dynamic is given by:

$$\dot{e}_3 = \frac{v_{dc}}{L_g} (2\boldsymbol{\beta 1} - 1) - \frac{R_g}{L_g} i_g - \frac{e_g}{L_g} - \frac{di_{gref}}{dt} \quad (21)$$

Consider the candidate Lyapunov function:

$$V_3 = \frac{1}{2} e^2{}_3$$

As its derivative with respect to time is given by:

$$\dot{V}_3 = e_3 \left[\frac{v_{dc}}{L_g} (2\boldsymbol{\beta 1} - 1) - \frac{R_g}{L_g} i_g - \frac{e_g}{L_g} - \frac{di_{gref}}{dt} \right] \quad (22)$$

The choice $-C_5 e_3 = \dot{e}_3$ with $C_5 > 0$ is a design parameter whose dynamics is negative definite.

$$-C_5 e_3 = \left[\frac{v_{dc}}{L_g} (2\boldsymbol{\beta 1} - 1) - \frac{R_g}{L_g} i_g - \frac{e_g}{L_g} - \frac{di_{gref}}{dt} \right] \quad (23)$$

We deduce the following backstepping stabilizing function:

$$\boldsymbol{\beta 1} = \left[-C_5 e_3 + \frac{R_g}{L_g} i_g + \frac{e_g}{L_g} + \frac{di_{gref}}{dt} \right] \frac{L_g}{2 v_{dc}} \quad (24)$$

3.3 MPPT ADRC Controller

To improve the response speed and control adaptability of the grid connected system [14], the applied ADRC method design is shown in fig.6. The main idea of this technology is to estimate and compensate the unmeasured state of the system or the total disturbance, in real time, even without an explicit model of the plant and only from the input-output information [9]. To ensure that, the controller contains three blocks: differentiator trackers (DT), feedback controller (FC), and extended state observer (ESO). It involves also an inner loop to reject the total disturbance and an outer one to deliver the desired signal.

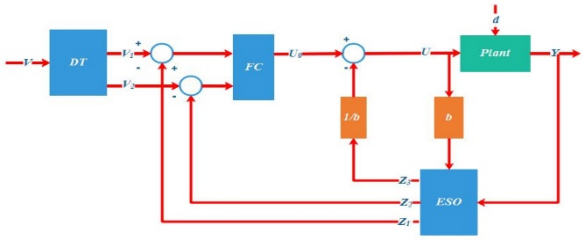

Fig. 6. ADRC controller structure.

As shown in fig.7, to extract the maximum power from the PV System, the ADRC controller is designed to set the following signal error at 0.

$$e = \frac{I}{V} + \frac{dI}{dV} \tag{25}$$

DT is used to arrange the transient process, and to get the differential signals of current *dI* and voltage *dV* with two differentiators' trackers.

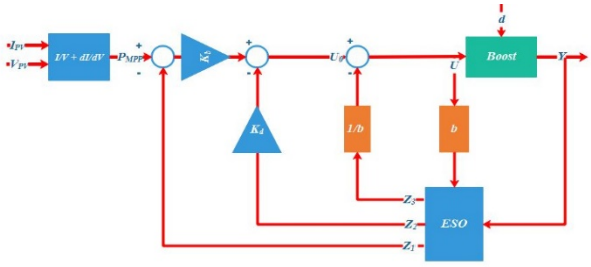

Fig. 7. MPPT based in ADRC controller.

It overcomes the drawback in the classical theory such as an amplificatory effect on the noise. Mathematical form is expressed by:

$$\begin{cases} \dot{X}_1 = X_2 \\ \dot{X}_2 = m\,\psi\left(X_1 - X + \frac{X_2|X_2|}{2m}\right) \end{cases} \tag{26}$$

Where m is the speed factor, X_1 and X_2 are respectively the tracking and differential output, X is the input signal and $\psi(.)$ is a nonlinear function.

ESO is the core part of ADRC, it contributes to get the model uncertainty and to deal with total disturbance affecting PV power system. Mathematical structure is given by:

$$\begin{cases} e = z_1 - y \\ \dot{z}_1 = z_2 - \theta_1 e \\ \dot{z}_2 = z_3 - \theta_2 e \\ \dot{z}_3 = -\theta_3 e \end{cases} \tag{27}$$

Where y is the output of the system. z_1, z_2 and z_3 are respectively the estimation of the output, the estimation of the derivative of the output and the estimation of the disturbance in system. Referring to [13], the observer gains $\theta_i (i = 1,2,3)$ are $3\omega_0$, $3{\omega_0}^2$, ${\omega_0}^3$. $K_P = {\omega_c}^2$, $K_d = 2\omega_c$ represent parameters of feedback controller (FC) which are used to generate the control input u_0.

ω_0 and ω_c are denoted as the bandwidth of the observer and the bandwidth of the feedback control.

Finally, the control law is:

$$u = \frac{u_0 - z_3}{b} \tag{28}$$

b is the disturbance compensation factor.

3.4 ADRC for grid side inverter

The voltage source inverter involves double closed loop. The external loop is responsible for DC-bus voltage and generating the reference current corresponding to the active power while the internal loop is responsible for grid current control.

Referring to fig.8 and fig.9, all quantities are adjusted by ADRC controller to obtain satisfactory parameters.

The positive parameter γ is adjusted by the ADRC control law.

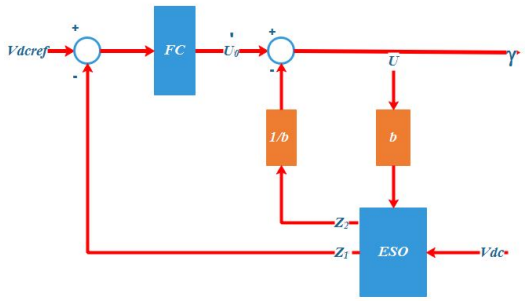

Fig. 8. DC Voltage based in ADRC Controller.

Side inverter is a third-order system, it can be transformed into cascade integral form.

$$\begin{cases} \dot{\bar{x}}_1 = \bar{x}_2 \\ \dot{\bar{x}}_2 = \bar{x}_3 \\ \dot{\bar{x}}_3 = f(\bar{x}_1, \bar{x}_2, \bar{x}_3, e_g) + bU''_0 \end{cases} \tag{29}$$

Where $\bar{x}_1, \bar{x}_2$ and $\bar{x}_3$ are the state variables.

Four-order ESO structure must be used to provide more robust observer dynamics as shown below:

$$\begin{cases} e = z_1 - \bar{x}_1 \\ \dot{z}_1 = z_2 - \lambda_1 e \\ \dot{z}_2 = z_3 - \lambda_2 e \\ \dot{z}_3 = f(z_1, z_2, z_3, e_g) + z_4 + bU''_0 - \lambda_3 e \\ \dot{z}_4 = -\lambda_4 e \end{cases} \quad (30)$$

By selecting the feedback coefficients λ_1, λ_2, λ_3, λ_4 properly, the estimation error converges to a small value.

$$\lambda_1 = 4\omega_0,\ \lambda_2 = 6{\omega_0}^2, \lambda_3 = 4{\omega_0}^3, \lambda_4 = {\omega_0}^4$$

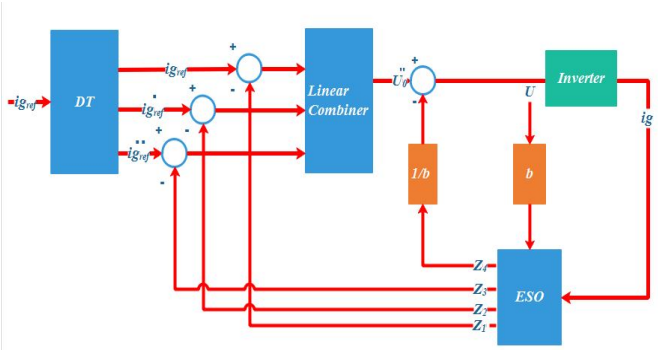

Fig. 9. Side inverter ADRC Controller structure.

4. Simulation and results and discussion

Simulation of the power system was carried out in MATLAB Simulink. As shown in fig.10, the system consists of 5 blocks, namely the PV model with its variable climate inputs, the model of the DC / AC converters with its parameters, and the two controllers based on the ADRC and Backstepping approach. Parameters used in power grid system and their command are mentioned in table 3. Performances and design results of the control system are illustrated throughout two cases. In the first scenario, realistic ramp up/down radiation from 1000w/m² to 300w/m² are applied while the temperature is kept constant at 298K. In the second case, the temperature changes its values as follows: 323K to 298K at t = 1.2s and from 298K returning to 323K at 1.8s meanwhile the radiation is maintained at 1000w/m².

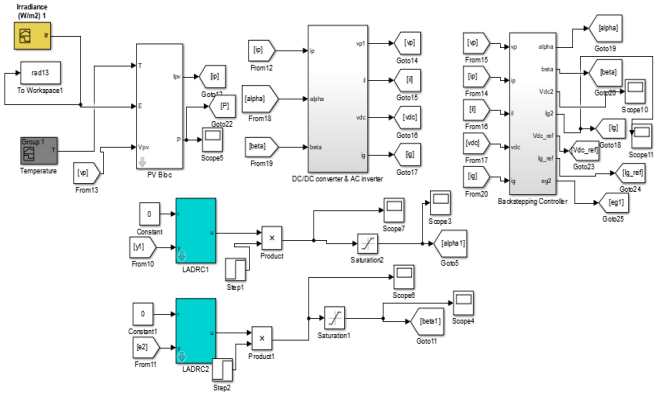

Fig. 10. Power grid connected system simulation.

Table 3. Characteristics of the Power System.

Power grid Characteristics	Backstepping parameters	ADRC parameters	
$C_{in} = 47mF$ $C_{dc} = 4.7mF$	$C_1 = 50$ $C_2 = 1000$	Boost converter	Side inverter
$L_g = 2.2mH$ $R_g = 0.47\Omega$	$C_3 = 200$	$\omega_0 = 440$	$\omega_0 = 240$
$L = 3.5mH$	$C_4 = 0.025$	$\omega_c = 110$	$\omega_c = 60$
$v_{dcref} = 25v$	$C_5 = 50$	$b = 600$	$b = 1500$

The resulting control performances of the first case is illustrated by fig. 11 to fig. 15 and for the second one is illustrated by fig. 16 to fig. 19. Figures 11 and 16 shows that the both commands deliver a control signal α which drive the boost converter to track the MPP very quickly. As illustrated the PV output power provides with variable climatic conditions the maximal power, which is equal 70w, and minimal power which is 20w, corresponding to the MPP P1 and P3 in fig. 4. Moreover, noting that in fig. 12 and fig. 17 the DC bus voltage v_{dc} is regulated to its reference value v_{dcref} =25V with good performance even with climate change in order to be used as constant input for inverter. Also, the PV current is set to its value and track the variation of climatic inputs. Additionally, the synchronization to the grid is ensured. Injected current tracks its reference grid value i_{gref}, grid current and voltage are sinusoidal and in phase, which guarantee that the PV grid connected system achieve the unity power factor. Finally, the control inputs of converter and inverter α and β are clearly bounded and as shown in fig. 15, the error tends to zero.

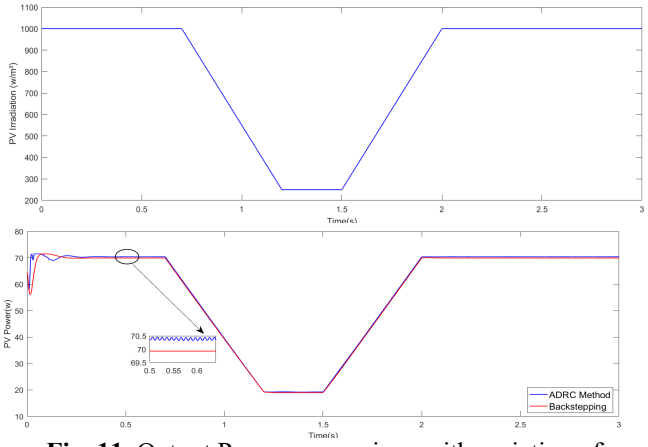

Fig. 11. Output Power comparison with variation of irradiation

According to figures, the backstepping command present excellent characteristics and good performances comparing to ADRC control technique which present especially at the beginning remarkable oscillations and high overshoot, and this is due to the time taken by the approach to transform the data of the problem using Simulink into a set of results. Otherwise, for an implementation the backstepping method requires more sensors, software and programming comparing

to ADRC method which is generally cheaper and less complex because it requires two tuning parameters to adjust.

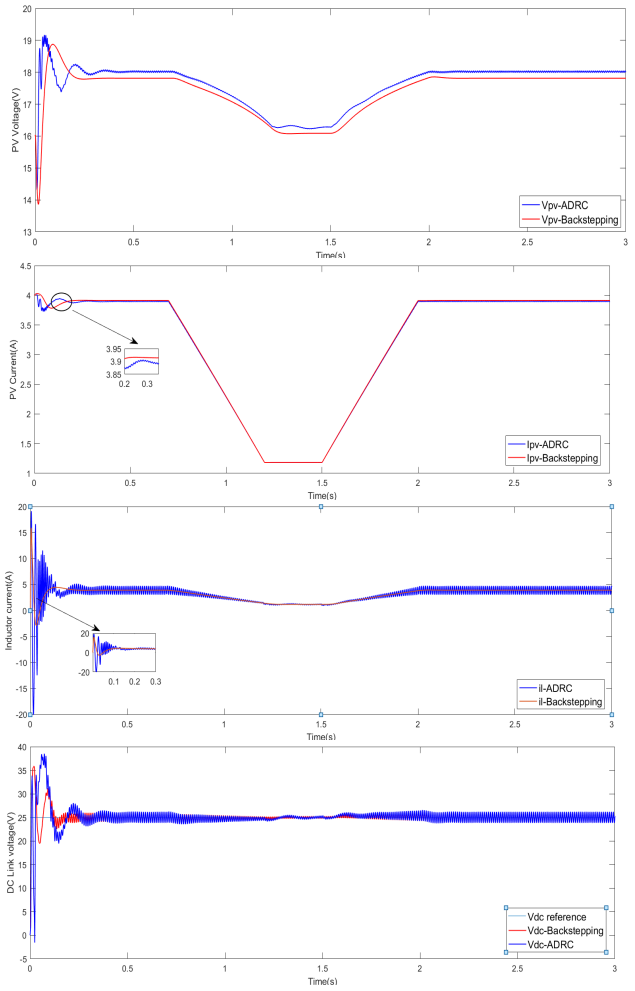

Fig. 12. PV voltage, PV current, inductor current, DC link voltage of the converter

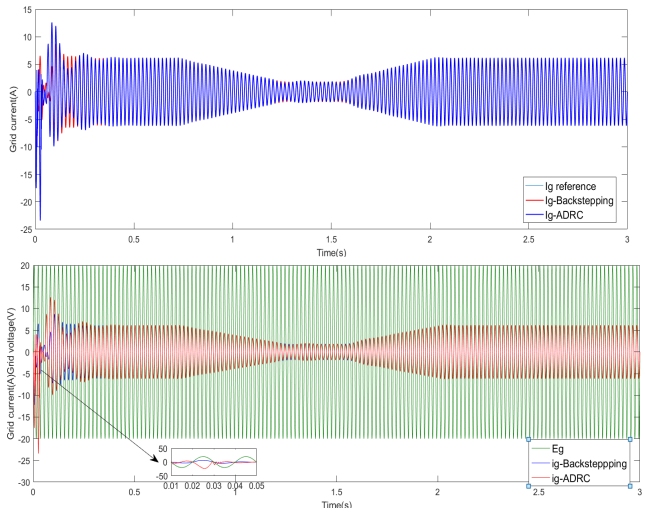

Fig. 13. PFC checking and grid current with its reference

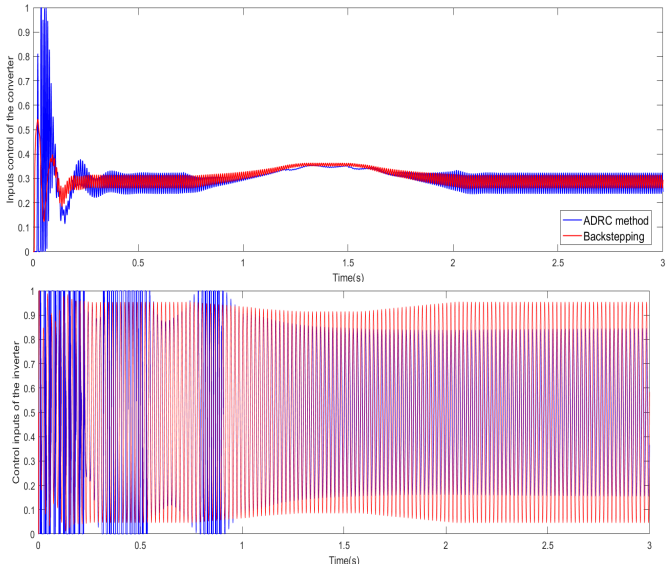

Fig. 14. Control signal comparison of the converter and inverter

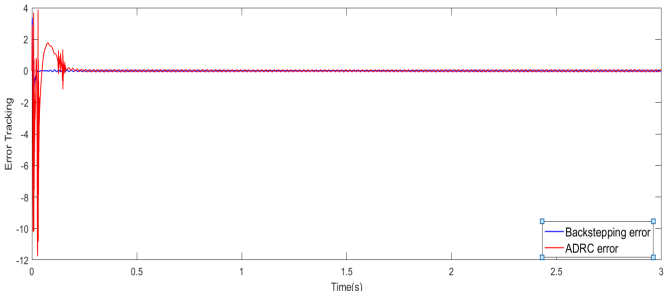

Fig. 15. Backstepping and ADRC command error

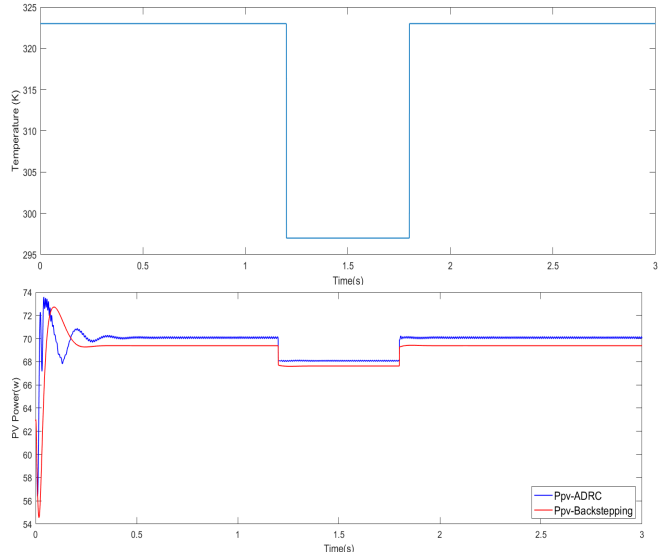

Fig. 16. Output Power comparison with variation of temperature

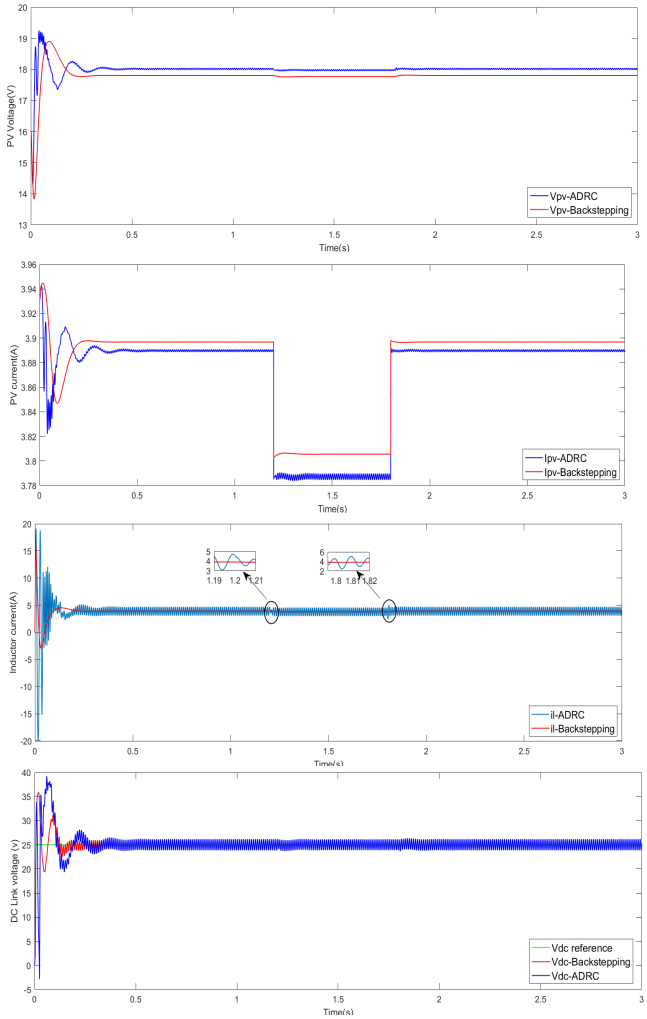

Fig.17. PV voltage, PV current, inductor current, DC bus voltage of the converter

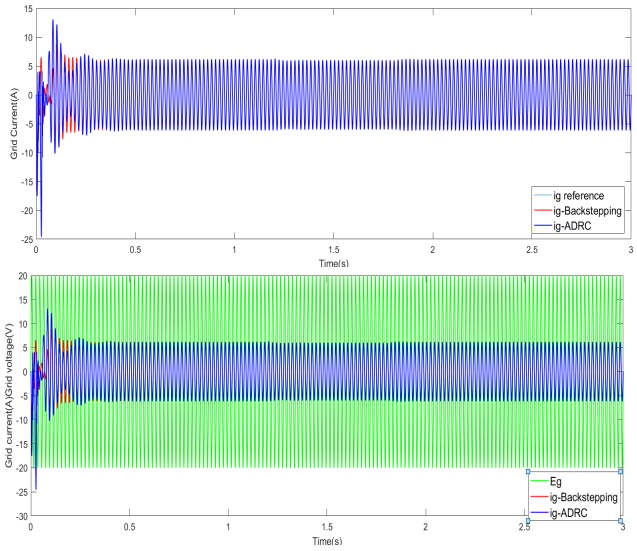

Fig.18. PFC checking and grid current with its reference

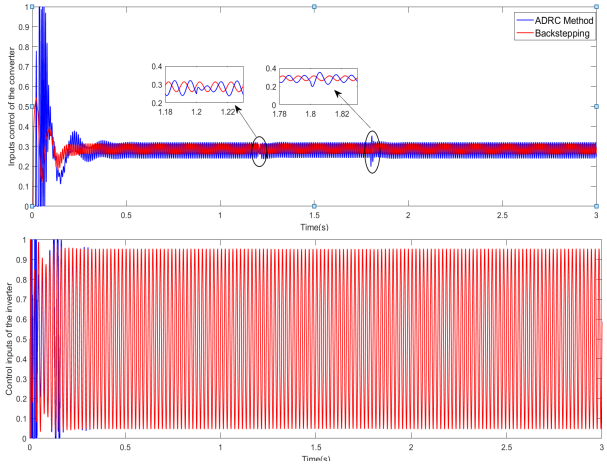

Fig.19. Control signal comparison of the converter and inverter

5. Conclusion

In this study, two control strategies for grid connected inverter were proposed to ensure a complete control of the PV system. Both controllers, backstepping and ADRC were developed to track the MPP, to regulate DC bus voltage and to get desired current waveform in phase with the grid voltage. The synthesis of the controllers was achieved respectively by using for the first one stability tools of Lyapunov and for the second by tuning two parameters using also different blocks. Simulation results show that the backstepping guarantees satisfactory characteristics with good efficiency and strong performance even with external disturbance and weather variations when comparing with ADRC method. Otherwise, with less parameters and especially for the tracking problem implementation, ADRC would be a technology worthy for try and easy to carry on. This work is expected to provide more ideas for the researchers to apply the ADRC in a real prototype for power electronic converters control. The comparison study indicates a promising prospect of ADRC in the future industry.

References

[1] N. Khaldi, H. Mahmoudi, M. Zazi, Y. Barradi, "Modelling and Analysis of Neural Network and Incremental Conductance MPPT Algorithm for PV Array Using Boost Converter" In: Proc. of the 3rd International Conference on Energy and Environment Technologies and Equipment (EEETE '14), Brasov, Romania, pp 148-153, June 26-28, 2014.

[2] M. Othman, Mahdi M. El-Arini, And Ahmed Fathy, "Real world Maximum Power Point Tracking Based on Fuzzy Logic Control", WSEAS Trans. on Power Systems, Vol. 9, pp 232-241, 2014.

[3] N. Khaldi, H. Mahmoudi, M. Zazi, Y. Barradi, "Implementation of a MPPT neural controller for photovoltaic systems on FPGA circuit", WSEAS Trans. on Power Systems, Vol. 9, pp 471-478, 2014.

[4] N. Khaldi, H. Mahmoudi, M. Zazi, Y. Barradi, " The MPPT Control of PV System by Using Neural Networks

Based on Newton Raphson Method", IEEE, the 2nd International Renewable and Sustainable Energy Conference (IRSEC '14) Ouarzazate, Morocco, pp1-6, October 17-19, 2014.

[5] I. Houssamo, F. Locment, M. Sechilariu, "Experimental analysis of impact of MPPT methods on energy efficiency for photovoltaic power systems", International Journal of Electrical Power & Energy Systems, Vol. 46, pp.98-107,2013.

[6] Y. J. M. Carrasco, L. G. Franquelo, J. T. Bialasiewicz, E. Galvan, R. C. Portillo Guisado, M. A. M. Parts, J. I. Leon and N. Moreno-Alfonso, "Power-electronic systems for the grid integration of renewable energy sources", A survey, IEEE T. Ind. Electron. 53, 2006.

[7] N. Khaldi, Y. Barradi, H. Mahmoudi, M. Zazi," Design and implementation of Backstepping controller for photovoltaic systems using an Arduino Board", International Journal of Renewable Energy research (IJRER), vol. 7, No. 2, pp 817-824, 2017.

[8] L. Sun, J. Dong, D. Li, and K. Y. Lee, "A practical multivariable control approach based on inverted decoupling and decentralized active disturbance rejection control," Industrial & Engineering Chemistry Research, Vol. 55, pp 2008–2019, 2016.

[9] S. Yi Huang, W. Zhang, ''Development of active disturbance rejection controller'', Control Theory & Applications, Vol. 19, pp 485-492, 2005.

[10] W. Zhenlong, W. Haisu, L. Donghai, T. Hg e , J. Fengsheng , L. Sun, "A comparison study of a high order system with different ADRC control strategies" IEEE, In Proc. of International Conference 37th Chinese Control , Wuhan, China, pp236-241, 2018.

[11] J.L. Yang, D.T. Su, Y.S. Shiao, "Research on MPPT and Single stage Grid-Connected for Photovoltaic System" WSEAS Transactions On Systems.Vol.7, pp. 1117–1131, 2008.

[12] H. Wang, X. Jin, H. Zhao, Y. Yue, ''MPPT Control Method of PV System Based on Active disturbance rejection Control'' IEEE, In Proc. of International Conference on Mechatronics and Automation, Takamatsu, Japan, pp337-341, 2017.

[13] Z. Gao, ''Scaling and Bandwidth-Parameterization based Controller Tuning'' In Proc. of the American Control Conference, Denver, CO, United States, Vol. 6, pp 4989-4996, 2003.

[14] K. M. Alawasa, A. I. AL-Odienat, "Power quality characteristics of residential grid connected inverter of photovoltaic solar system" IEEE 6th International Conference on Renewable Energy Research and Applications (ICRERA), USA, pp.1097-1101, November, 2017.

[15] A. Del Pizzo, L. P. Di Noia, M. Santolo, "Super twisting sliding mode control of smarts inverters grid connected for PV applications " IEEE 6th International Conference on Renewable Energy Research and Applications (ICRERA), USA, pp. 793-796, November, 2017.

[16] T. Ming Tsung, L. Ching Lung, M. Wei Cong, "Implementation of a serial AC/DC converter with modular control technology " IEEE 7th International Conference on Renewable Energy Research and Applications (ICRERA), France, pp. 245-250, October, 2018.

[17] Y. Soufi, S. Kahla, M. Sedraoui, M. Bechouat "Optimal control based RST controller for maximum power point tracking of wind energy conversion system" IEEE 5th International Conference on Renewable Energy Research and Applications (ICRERA), UK, pp. 1168-1172, November, 2016.

[18] I. Keskin, G. Soykan, "Reduction of peak power consumption by using photovoltaic panels in Turkey" IEEE 6th International Conference on Renewable Energy Research and Applications (ICRERA), USA, pp. 886-890, November, 2017.